in planktonic environments coupled with biological processes of selective feeding, digestion, and degradation during pellet formation and deposition, provide an array of organic compounds as diverse as the ecosystems that produced them. This chemical diversity of potential petroleum precursors can explain, in part, the variety of hydrocarbon compounds found in crude oils. The pellets are also a major source of phosphate that later is available to precipitate into nodules. The specific environments in which pellet-rich banded sediments are being produced today may provide depositional stratigraphic models for future fossil fuel and mineral resource discovery and for the simulation of hydrocarbon-producing food chains.

KAREN GLAUS PORTER
Department of Zoology and
Institute of Ecology,
University of Georgia, Athens 30602
ELEANORA IBERALL ROBBINS
U.S. Geological Survey,
Reston, Virginia 22092

References and Notes

1. Samples are from the Bandera Shale Member of the Oologah Formation and the Excello Shale Member of the Senora Formation collected from roadcuts east of Tulsa, Oklahoma; the Meade Peak Phosphatic Shale Member of the Phosphoria Formation collected from Mabie Canyon, Snowdrift Mountain, and Bloomington Canyon, Idaho, and Sublette Ridge and Coal Canyon, Wyoming; the Cumnock Formation collected from BMDH D-1 core hole from a depth of 156.7 m, north of Cumnock, North Carolina; and the Puente Formation collected from Union Oil Company well, Bell 107, in two samples between 3831 and 3957 m, Santa Fe Springs, California. For quantitative analysis, 10-g pieces of whole shale and nodules were treated at 22°C with 10 percent HCl for 24 hours, rinsed three times with distilled water, settled by gravity, and treated with 50 percent hydrofluoric acid for 24 hours. Samples were then rinsed five times with distilled water and passed through a 125-μm sieve and then a 25-μm sieve. Subsamples of the microfossil fraction were measured and counted at magnifications of 100 to 1000. Standard use of hot acid, centrifugation, hydroxide, and Shultze solution will destroy pellet remains. Thin sections of shale samples were examined qualitatively. The complete technique is described by E. I. Robbins and A. Traverse, in *Carolina Geologic Society Guidebook* (Savannah River Laboratory, Aiken, S.C., 1980), section B, p. 1.
2. Details of microfossil analyses, reconstructions of the paleoenvironments, and the economic importance of the formations are described by E. I. Robbins and K. G. Porter, in preparation.
3. H. A. Tourtelot, *Clays Clay Miner.* **27**, 313 (1979).
4. E. I. Robbins and K. G. Porter, *Palynology* **4**, 30 (1979).
5. Standard chemical analyses were performed by N. G. Skinner and Z. A. Hamlin, U.S. Geological Survey. The percent by weight of the intact pellet in the total sample was calculated by weighing the microfossil fraction (> 25 μm) and multiplying this weight by the intact pellet percent by volume.
6. R. E. Johannes and M. Satomi, *Limnol. Oceanogr.* **11**, 191 (1966).
7. S. Honjo, *J. Mar. Res.* **38**, 53 (1980).
8. J. T. Turner and J. C. Ferrante, *BioScience* **29**, 670 (1979); S. Honjo and M. R. Roman, *J. Mar. Res.* **36**, 45 (1978).
9. H. B. Moore, *J. Mar. Biol. Assoc. U.K.* **17**, 325 (1931); *ibid.*, p. 359; A. J. Iovino and W. H. Bradley, *Limnol. Oceanogr.* **14**, 898 (1969).
10. K. G. Porter, *Verh. Int. Ver. Theor. Angew. Limnol.* **19**, 2840 (1975); *Science* **192**, 1332 (1976); *Am. Sci.* **65**, 159 (1977); S. A. Poulet, *Limnol. Oceanogr.* **23**, 1126 (1978).
11. R. Conover, *J. Fish. Res. Board Can.* **28**, 1327 (1971); F. G. Prahl and R. Carpenter, *Geochim. Cosmochim. Acta* **43**, 1959 (1979); J. R. Syvitski and A. G. Lewis, *J. Sediment. Petrol.* **50**, 869 (1980).
12. S. Honjo, *J. Mar. Res.* **36**, 469 (1978).
13. H. B. Moore, in *Recent Marine Sediments*, D. D. Trask, Ed. (American Association of Petroleum Geologists, Tulsa, Okla., 1939), p. 516; D. E. Hattin, *J. Sediment. Petrol.* **45**, 1 (1975); A. Soutar, S. A. Kling, P. A. Crill, D. Duffrin, K. W. Bruland, *Nature (London)* **266**, 136 (1977); G. Knauer, J. H. Martin, K. W. Bruland, *Deep-Sea Res.* **26A**, 97 (1979); B. Hargrave, in *Marine Benthic Dynamics*, K. R. Tenore and B. C. Coull, Eds. (Belle W. Baruch Library in Marine Sciences, Columbia, S.C., No. 11, 1980), p. 243.
14. D. C. Rhoads and J. W. Morse, *Lethaia* **4**, 413 (1971).
15. G. J. Demaison and G. T. Moore, *Org. Geochem.* **2**, 9 (1980).
16. M. Brongersma-Sanders, *Mar. Geol.* **11**, 123 (1971); A. P. Bennison, *Tulsa Geol. Soc. Dig.* **37**, 1125 (1972); R. Zangrel and E. S. Richardson, Jr., *Fieldiana Geol. Mem.* **4**, 1 (1963).
17. M. M. Cassidy, *Bull. Am. Assoc. Pet. Geol.* **52**, 295 (1968); G. W. James and D. R. Baker, *Kans. State Geol. Surv. Bull.* **204**, 3 (1972).
18. P. E. Olsen, C. L. Remington, B. Cornet, K. S. Thomson, *Science* **201**, 729 (1978).
19. R. P. Sheldon, *U.S. Geol. Soc. Prof. Pap. 313-B* (1963), p. 1; R. A. Gulbrandsen, *ibid. 550-D* (1966), p. D-199; V. E. McKelvey, *Bull. U.S. Geol. Surv. 1252-D* (1967); E. K. Maughan, in *Proceedings of the International Conference of Comparative Geology of Phosphate and Oil Deposits* (Bureau de Recherches Geologiques et Minieres, Orleans, France, 1980), p. 63.
20. We thank V. E. McKelvey, G. L. Bain, L. E. Eames, and T. H. McCulloh for samples and C. W. Byers, R. R. Cohen, E. R. Force, S. Honjo, G. E. Hutchinson, T. M. Kehn, M. L. Pace, J. S. Patton, J. W. Porter, D. Rhoads, T. M. Schopf, S. Stanley, and G. A. Younse for their comments on the manuscript. Contribution No. 6 of the Lake Oglethorpe Limnological Association.

21 January 1981

Didemnins: Antiviral and Antitumor Depsipeptides from a Caribbean Tunicate

Abstract. *Extracts of samples of a Caribbean tunicate (ascidian, sea squirt) of the family Didemnidae inhibit in vitro at low concentrations the growth of DNA and RNA viruses as well as L1210 leukemic cells. The active compounds isolated from the tunicate, didemnins A, B, and C, are depsipeptides, and didemnin B (a derivative of didemnin A) is the component active at the lowest concentration in inhibiting viral replication in vitro and P388 leukemia in vivo.*

We have isolated from a Caribbean tunicate a new class of depsipeptides, including highly active antiviral and antitumor agents (*1*). Although these depsipeptides—termed didemnins after the name of the tunicate family from which they are isolated—are closely related to one another, they vary in activity, suggesting the possibility of further chemical modification. This discovery confirms our earlier observations (*2*, *3*) that the subphylum Tunicata or Urochordata (phylum Chordata) is of special interest both for the chemistry and for the bioactivity of the compounds tunicates contain (*4*, *5*).

The tunicate in our study was collected at a number of sites (including Colombian, Honduran, Mexican, Belizean, and Panamanian waters) during the *Alpha Helix* Caribbean Expedition 1978 (AHCE 1978) (*3*). It has been assigned (*6*) to the family Didemnidae and is a member of the *Tridemnum* genus. Repeated tests of methanol-toluene (3:1) extracts of the didemnid on shipboard against herpes simplex virus, type 1, grown in CV-1 cells (monkey kidney tissue) indicated that it inhibited the growth of the virus, over and above an underlying cytotoxicity to the CV-1 cells. This result suggested that compounds in the tunicate extract offered promise both as antiviral agents and,

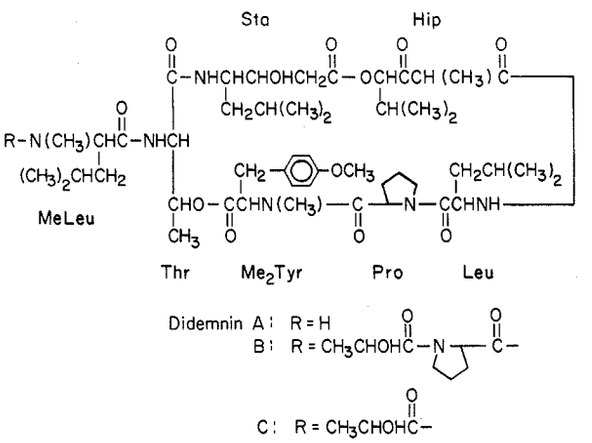

Fig. 1. Structures of didemnins.

0036-8075/81/0522-0933$00.50/0

potentially, as antitumor agents as well.

Extracts of the tunicate collected at a number of sites were subsequently tested against other viruses. Essentially all of the extracts, regardless of the collecting site, showed activity in inhibiting both RNA and DNA viruses (Table 1). At 1 mg/ml the extracts were also cytotoxic to the cells infected by the viruses, but at 250 μg/ml the cytotoxicity generally disappeared. In addition, the suggestion that the extracts might also have antitumor properties received support from their high potency against L1210 murine leukemic cells.

Isolation and separation of the compounds responsible was effected by partitioning the methanol-toluene extracts with aqueous sodium nitrate, extracting the aqueous layer with chloroform, concentrating the chloroform layer, and chromatographing over silica gel with a step gradient of methanol in chloroform to give didemnins C, B, and A (in order of elution), which could be further purified by preparative thin-layer chromatography with the same system. Didemnins A, B, and C contain both the antiviral activity and the cytotoxicity of the crude extracts (Table 1).

More detailed studies of didemnins A and B are provided in Tables 2 and 3. Didemnins A and B are both potent antiviral agents. Less than about 1 μ*M* didemnin A and about 0.05 μ*M* didemnin B effected a 1-log reduction in titers of herpes simplex virus, types 1 and 2, whereas adenosine arabinoside, a clinical antiviral agent, was reported earlier to effect 1-log reductions in titers of the same viruses at levels above 10 μ*M* (*7*). Didemnin B inhibits the five viruses at concentrations 10- to 100-fold lower than does didemnin A. However, it is also more cytotoxic toward the mammalian cells tested and the relative efficacy (if any) of the two didemnins as antiviral agents must await results of in vivo studies. Initial results indicate protection of mice from vaginal herpes simplex, type 2, infections by both didemnins A and B (*8*).

With respect to antitumor activity, the concentration of didemnin B required for 50 percent inhibition of L1210 cell growth is only 0.001 μg/ml, while that of didemnin A is more than ten times higher (Table 1). The higher potency of didemnin B is also reflected in its in vivo antitumor activity. As shown in Table 3, the dosage level of didemnin B required to increase the life-span of P388 leukemia–bearing mice by 40 percent is only about 1 percent of that required for didemnin A (0.06 mg/kg compared to 8 mg/kg). More importantly, didemnin B extends the survival time of tumor-bearing mice by about twofold (test/control = 199) when the animals are given intraperitoneal injections of the drug (1 mg/kg) on days 1, 5, and 9 after tumor inoculation. Thus, didemnin B is a promising antitumor drug candidate and warrants further development. Although the dose of didemnin A required for achieving a comparable therapeutic effect is higher than that for didemnin B, the

Table 1. Bioactivities of didemnid tunicate (*Tridemnum* sp.) extracts and of didemnins. The activities are expressed as the relation of zones of cytotoxicity to zones of virus inhibition (zones of inhibition: 1 = 1 to 10 mm, 2 = 10 to 20 mm, 3 = 20 to 30 mm, and 4 = 30 to 40 mm) for 20 μl of solutions containing 1 mg of sample per milliliter.

Test material*	AHCE sample†					Didemnins		
	C	H	M	B	P	A	B	C
				DNA antiviral assays				
HSV-1	2/4	1/2	1/4	1/4	2/4			
HSV-2	2/4	1/3	1/4	1/4	2/4	2/3	3/3	2/3
Vaccinia virus	1/4	0/3	1/4	1/4	2/4			
				RNA antiviral assays				
PR8	2/0	2/3	2/4	0/0	4/4			
HA-1	1/3	3/4	1/3	0/2	3/4			
COE	2/3	3/4	2/0	0/2	4/0			
ER	2/4	2/4	3/4	1/2	3/0			
				Cytotoxicity ID_{50} (μg/ml)‡				
L1210	0.015	0.16	0.20	0.26	N.T.§	0.019	0.0011	N.T.‡

*HSV-1, HSV-2 (herpes simplex virus, types 1 and 2), vaccinia virus, all grown in primary rabbit kidney cells; PR8 (influenza virus) was grown in embryonic chick kidney cells; HA-1 (parainfluenza-3 virus) was grown in Hep-2 (human epidermal carcinoma) cells; COE (Coxsackie A-21 virus) and ER (equine rhinovirus) were grown in ML (a variant of HeLa cervical carcinoma) cells. †C, Colombia; H, Honduras; M, Mexico; B, Belize; and P, Panama. ‡ID_{50}, inhibitory dose. §N.T., not tested.

Table 2. Virus titers in absence and presence of didemnins A and B.

Drug	Concentration (μg/ml)	Virus titers, PFU/0.2 ml*				
		COE	ER	HA-1	HSV-1	HSV-2
None†	0	1.9×10^4	1.2×10^3	6.1×10^2	3.1×10^3	9.0×10^1
None	0	6.5×10^7	2.5×10^6	1.2×10^6	2.0×10^7	1.5×10^6
Didemnin A‡	50	2.9×10^3	$< 10^1$	$< 10^1$	2.2×10^2	$< 10^1$
	5	1.8×10^3	1.7×10^2	4.0×10^1	2.7×10^5	2.4×10^4
	0.5	1.6×10^6	1.7×10^4	9.9×10^2	1.8×10^7	9.3×10^5
	0.05	5.7×10^7	2.1×10^6	2.3×10^5	2.2×10^7	1.5×10^6
Didemnin B§	50	8.5×10^2	$< 10^1$	$< 10^1$	$< 10^1$	$< 10^1$
	5	1.6×10^3	4.5×10^1	$< 10^1$	2.0×10^2	$< 10^1$
	0.5	1.6×10^3	2.5×10^2	6.3×10^1	2.1×10^2	9.5×10^2
	0.05	1.5×10^7	3.6×10^4	1.4×10^3	2.5×10^6	1.0×10^5

*Plaque-forming units 24 hours after inoculation of cells with virus and drug. Virus abbreviations are the same as in Table 1, except that HSV-1 and HSV-2 were grown in Vero cells (a serially propagated monkey kidney cell line). †Time zero. ‡The inhibitory dose (ID_{50}) was 25 μg/ml (ML cells) and 50 μg/ml (Vero cells). §The ID_{50} was < 1.5 μg/ml (ML cells) and 12 μg/ml (Vero cells).

Table 3. In vivo activities of didemnins A and B against P388 leukemia in mice.

Dose (mg/kg)*	Weight change (g)		Median survival time (days)†		T/C‡ (%)	
	A§	B§	A	B	A	B
0.03		+1.6		12.8		125
0.06		+1.2		14.3		140
0.12		+0.2		15.0		147
0.25	+1.7	−0.5	11.1	16.0	109	157
0.5	+1.6	−1.7	12.1	18.0	118	176
1	+1.8	−3.8	12.1	20.3	118	199
2	+2.0		12.4		121	
4	+1.3		13.3		130	
8	+0.8		14.3		140	

*Per injection, on days 1, 5, and 9, intraperitoneally. Tumor cell inoculation on day zero. †The median survival time of control animals (without drug) was 10.2 days. ‡Test/control. §A, didemnin A; B, didemnin B.

former is still a very potent drug; however, because of a scarcity of sample, didemnin A has not yet been evaluated at optimum dosage levels for its antitumor effect in vivo. Didemnin C, the trace component, has not been available in quantities adequate for extensive testing.

Interest in the chemotherapeutic potential of the didemnins is heightened by recent investigations (*9*) resulting in the structure elucidation of didemnins A, B, and C (Fig. 1). Novel aspects are a new structural unit for depsipeptides, hydroxyisovalerylpropionate, and a new stereoisomer of the highly unusual amino acid statine. It is particularly noteworthy that didemnins B and C are simple derivatives of didemnin A. That the biological activities of the didemnins can be dramatically altered by slight chemical changes bodes well for the development of a useful therapeutic agent.

KENNETH L. RINEHART, JR.
JAMES B. GLOER
Roger Adams Laboratory,
University of Illinois, Urbana 61801
ROBERT G. HUGHES, JR.
Department of Cell and Tumor Biology,
Roswell Park Memorial Institute,
Buffalo, New York 14263
HAROLD E. RENIS
J. PATRICK MCGOVREN
EVERETT B. SWYNENBERG
DALE A. STRINGFELLOW
SANDRA L. KUENTZEL
LI H. LI
Upjohn Company,
Kalamazoo, Michigan 49001

References and Notes

1. Presented in part at the 3rd International Symposium on Marine Natural Products (International Union of Pure and Applied Chemistry and Société Chimique de Belgiques), Brussels, 16 September 1980.
2. P. D. Shaw, W. O. McClure, G. Van Blaricom, J. Sims, W. Fenical, J. Rude, in *Food-Drugs from the Sea Proceedings 1974*, H. H. Webber and G. D. Ruggieri, Eds. (Marine Technology Society, Washington, D.C., 1976), pp. 429–433; K. L. Rinehart, Jr., R. D. Johnson, I. C. Paul, J. A. McMillan, J. F. Siuda, G. E. Krejcarek, *ibid.*, pp. 434–442.
3. K. L. Rinehart, Jr., *et al.*, *Pure Appl. Chem.* **53**, 795 (1981).
4. M. T. Cheng and K. L. Rinehart, Jr., *J. Am. Chem. Soc.* **100**, 7409 (1978).
5. G. T. Carter and K. L. Rinehart, Jr., *ibid.*, p. 7441.
6. By Dr. Françoise Lafargue, Laboratoire Arago, Banyuls-sur-mer, France, and Dr. Charles C. Lambert, Department of Biological Science, California State University, Fullerton.
7. H. E. Renis, *Antimicrob. Ag. Chemother.* **11**, 701 (1977); *ibid.* **13**, 613 (1978).
8. _____, unpublished data.
9. K. L. Rinehart, Jr., J. B. Gloer, J. C. Cook, Jr., S. A. Mizsak, and T. Scahill, *J. Am. Chem. Soc.* **103**, 1857 (1981).
10. Supported in part by grants from the National Institute of Allergy and Infectious Diseases (AI 04769), the National Institute of General Medical Sciences (GM 27029), and from the National Science Foundation (PCM 77-12584). We thank the governments of Colombia, Honduras, Mexico, Belize, and Panama for permission to carry out scientific research in their territorial waters.

22 September 1980; revised 6 February 1981

Gated Sodium-23 Nuclear Magnetic Resonance Images of an Isolated Perfused Working Rat Heart

Abstract. *Sodium-23 nuclear magnetic resonance images of phantoms and gated images of isolated perfused working rat hearts were obtained. By synchronizing the nuclear magnetic resonance process to the heartbeat, images were obtained at systole and at diastole.*

Since its inception (*1*), nuclear magnetic resonance (NMR) imaging has progressed from a curiosity to the point where it promises to become one of the more important diagnostic tools in medicine. Several examples of high-resolution (millimeter) NMR images of protruding appendages of the human body, notably limbs and heads, have been published (*2–4*). Technological progress is being made, and NMR images of cross sections of the human torso may soon have a resolution comparable to that now obtained for heads and limbs. It is important that methods for using NMR imaging as a noninvasive diagnostic modality in cardiovascular research be developed.

Gating the acquisition of NMR signals to the heartbeat (*5*) was essential in our experiment in order to overcome the problems posed by heart motion. In addition to developing NMR technology suitable for imaging a beating heart, the physiological basis for providing contrast between the heart and the blood must be identified. Proton NMR images based on proton density alone may provide little contrast between blood and surrounding tissues. However, there is a significant difference between the concentration of sodium in blood and that in healthy tissue. We sought, therefore, to produce ^{23}Na NMR images of the heart. They would be negative images of the myocardium inasmuch as healthy tissue has a low sodium content compared to blood.

For these experiments, we modified a Nicolet wide-bore NT 360 spectrometer (8.45 T) so that it would perform as an imaging instrument. This involved the addition of three computer-controlled digital-to-analog converters to vary the currents of the first-order gradient shim coils, and the composition of several routines to provide these controls during acquisition of NMR data and to allow reconstruction and display of images. The imaging method used was basically the projection reconstruction method (*1*) with the image plane defined by an adaptation of the *z*-gradient oscillation method. The thickness of the slice was established experimentally by use of a phantom consisting of a flat-bottom NMR tube with a thin layer (1 mm) of 100 m*M* NaCl on the bottom. By moving this phantom in the probe with the oscillating *z* gradient on, the thickness of the imaged slice was found to be about 1.5 mm. The acquisition of each free-induction decay was triggered from the aortic pressure wave. A delay between the trigger from the pressure wave and acquisition is programmed in order to choose the instant within the cardiac cycle at which the acquisition is triggered.

As has traditionally been the case, the image-producing system was validated by making ^{23}Na images of phantoms. Figure 1a shows a diagram of the cross section of a phantom that consisted of a 20-mm outer diameter NMR tube filled with distilled water, into which were placed 5- and 2-mm outer diameter tubes containing 145 m*M* NaCl. Figure 1b is the ^{23}Na NMR image of this phantom (obtained at 95.25 MHz) resulting from 12 projections in the *x-y* plane and reconstructed by the standard back-projection method. Each projection required averaging of 320 free-induction decays. The images shown in this report are defined by a matrix of 64 by 64 pixels and were photographed from the screen of a Hewlett-Packard 1304A, producing (unfortunately) minimal levels of contrast.

We obtained images of an isolated perfused working rat heart, using the perfusion apparatus previously described (*5*). The only modification was that the suction cannula was raised so that the level of perfusate in the NMR tube was above the heart. Since the perfusate (modified Krebs-Henseleit bicarbonate, *p*H 7.24) has a high sodium content, its presence external to the heart provided contrast to the ventricular wall. Gated planar images were obtained of a midventricular slice of the isolated working heart of a 350-g Sprague-Dawley rat (Fig. 2). These images were reconstructed from 12 projections, each projection obtained by averaging 320 free-induction decays. Since the spin-lattice relaxation time of sodium is short (approximately 40 msec) in tissue, acquisitions can be closely spaced. One free-induction decay can be collected during each heartbeat (approximately 230 msec). Thus each image required

0036-8075/81/0522-0935$00.50/0